EUROPEAN SYNCHROTRON RADIATION FACILITY

INSTALLATION EUROPEENNE DE RAYONNEMENT SYNCHROTRON

ESRF

Experiment Report Form

The double page inside this form is to be filled in by all users or groups of users who have had access to beam time for measurements at the ESRF.

Once completed, the report should be submitted electronically to the User Office via the User Portal:

https://wwws.esrf.fr/misapps/SMISWebClient/protected/welcome.do

Reports supporting requests for additional beam time

Reports can be submitted independently of new proposals – it is necessary simply to indicate the number of the report(s) supporting a new proposal on the proposal form.

The Review Committees reserve the right to reject new proposals from groups who have not reported on the use of beam time allocated previously.

Reports on experiments relating to long term projects

Proposers awarded beam time for a long term project are required to submit an interim report at the end of each year, irrespective of the number of shifts of beam time they have used.

Published papers

All users must give proper credit to ESRF staff members and proper mention to ESRF facilities which were essential for the results described in any ensuing publication. Further, they are obliged to send to the Joint ESRF/ ILL library the complete reference and the abstract of all papers appearing in print, and resulting from the use of the ESRF.

Should you wish to make more general comments on the experiment, please note them on the User Evaluation Form, and send both the Report and the Evaluation Form to the User Office.

Deadlines for submission of Experimental Reports

- 1st March for experiments carried out up until June of the previous year;
- 1st September for experiments carried out up until January of the same year.

Instructions for preparing your Report

- fill in a separate form for each project or series of measurements.
- type your report, in English.
- include the reference number of the proposal to which the report refers.
- make sure that the text, tables and figures fit into the space available.
- if your work is published or is in press, you may prefer to paste in the abstract, and add full reference details. If the abstract is in a language other than English, please include an English translation.

Aim & Research Questions

We aimed to understand how otolith properties (shape, weight) and different types of swimbladder-ear connections affect otolith motion in modern bony fishes. We specifically asked whether

1) the needle-shaped otolith in goldfish moves dominantly along the axis of sound presentation?
2) different types of swimbladder-ear connections such as gas-filled anterior extensions in the cichlid *Etroplus canarensis* and the "bony" Weberian apparatus in goldfish affect otolith motion?
3) distance and angle between left and right otoliths affect otolith motion?

Material & Methods

Test subjects: Freshly euthanized individuals of two species, namely goldfish (*Carassius auratus*; N=9) and the Canara pearlspot (*Etroplus canarensis*; N=10) were subjected to a 0.2 or a 0.5 kHz pure tone stimulus, respectively. Goldfish is characterized by an <u>indirect</u> swimbladder-ear connection in which a chain of ossicles and ligaments (= Weberian apparatus) links the swimbladder to the ears [1]. In *E. canarensis*, the swimbladder <u>directly</u> contacts the ears via anterior extensions [2,3]. Both species are so-called "hearing specialists" which display improved hearing abilities compared to species without swimbladders or species that lack any otophysic connection [4,5].

Improved setup: Standing wave tube-like setup (2D radiography)

In our last project (LS-2539), we found that the sound field in the tank including the small underwater speaker (Daravoc) was complex and clearly deviated from theoretical expectations [6]. Hence, we developed a standing wave tube-like setup that should disentangle the particle motion and pressure components of sound. This was achieved by using a horizontal tube that was equipped with a projector (miniature inertial shaker) at each end of the tank (Fig. 1A). These projectors can be either driven in phase (0°) creating a pressure maximum in the center of the tank or maximum particle motion occurs when the projectors are driven out of phase at 180° (Fig. 1B). In acoustics, standing wave tubes are generally made of a steel tube with a wall thickness >1 cm to avoid compliance effects [7]. To match, however, the requirements of the X-ray imaging, we performed 2D radiography in a plexiglass cylinder with a wall thickness of 5 mm and an enclosed water body of ca. 2L.

Sound stimulus: The stimulus was generated in the software CoolEdit 2000 composed of two silent periods (each with a duration of 1-3 sec) enclosing the actual sound stimulus (5 sec). The 0.2 kHz stimulus was presented at four to 19 different steps, i.e. at sound pressure levels (SPLs) ranging from 141 up to >177 dB re 1 μPa. The 0.5 kHz stimulus was presented at three different steps with SPLs ranging from 159 to >177 dB re

1 µPa. In the hutches at ID17 and ID19, the background noise (ID17: 116 dB re 1 µPa; ID19: 118 dB re 1 µPa) was distinctly lower than the SPLs measured during sound presentation. At the same sound step, the "in phase mode", i.e. maximum sound pressure and the "out of phase mode", i.e. maximum particle motion, differed at 14-26 dB.
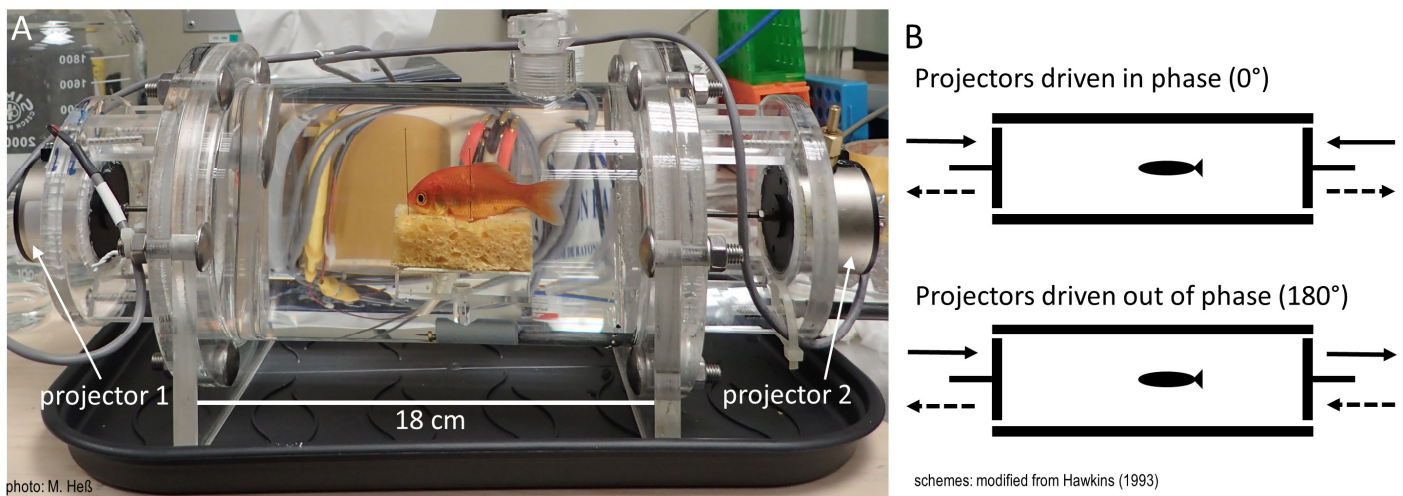

Fig. 1. (A) The new standing wave tube-like setup equipped with a projector (= miniature inertial shaker) at each end of the cylindrical Plexiglas® tank. (B) Driving the two projectors in phase (0°) creates a pressure maximum at the center of the tank whereas particle motion is maximal when the projectors are driven out of phase (180°, see [8]).

2D radiography (ID17 & ID19):
The fish was placed in the tank with its head located in the center of the tank. Imaging was performed with the fish seen in dorsal, lateral, and frontal views; the latter was performed in two specimens of *E. canarensis*. In dorsal and lateral views, the sound impinged along the rostrocaudal axis of the fish whereas in frontal view, sound impinged on the body flanks of the animal. The fish rested on a piece of foam that was glued to a Plexiglas® holder. To provide as many degrees of freedom for the fish's body to move in the sound field, it was fixed to the foam with two or three insect pins that were pierced subcutaneously through the body flanks and through the anterior most portion of the upper and lower jaws. Motion of the structures was captured with an image acquisition rate of 98.9954 fps (ID17) or 198.02 fps (ID19) when presenting the 0.2 kHz stimulus and 99.9028 fps (ID17) or 497.512 fps (ID19; only once: 99.900 fps) for the 0.5 kHz stimulus. In all cases, the integration time was 1 ms with a pixel size of 6.1 µm (ID17) or 3.67 µm (ID19), respectively. Images were recorded as 32-bit raw files (ID17) or 16-bit tif-files (ID19) with an effective average energy of 70 keV (ID17) or 59.2 keV (ID19). Motion at certain landmarks (squares of 40×40 pixels) was analyzed on background-corrected image stacks using the ImageJ plugin "Template matching – Align slices in stack" (see Fig. 2A).

Tomography (ID17):
One specimen of *E. canarensis* and one goldfish were subjected to a CT scan without sound presentation in order to identify and correctly assign structures seen in the 2D radiographs. We also performed CT scans in additional two individuals of *E. canarensis* and one goldfish focusing on the swimbladder in 3D comparing the condition 1) with presentation of a continuous 0.2 kHz pure tone stimulus to that of 2) no sound presentation. For this purpose, we used an upright 2L- Plexiglas® cylinder in which a small underwater speaker (Daravoc) was suspended from above. The fish was put with its snout pointing downwards into a 40mL plastic tube without cap in which the animal was stabilized with tissue and foam. The tube was glued to a metal holder placed in the center of the tank. Per scan (180° rotation), 2,600 images with a pixel size of 6.1 µm and at 14.444 steps per 1° were taken resulting in an image acquisition rate of 6.94 fps.

Results & Discussion
Successful separation of particle motion and pressure components of sound:
Measurements of sound pressure and particle acceleration levels using a miniture hydrophone or a p-a-sensor showed that levels between the in phase (0°) and out of phase (180°) condition differed at ca. 20 dB. As the gas-filled swimbladder in both species only displayed distinctly oscillating walls during the in phase condition, this indicates that the new setup allows for a successful separation between the two sound

components. However, the separation is not complete and might be further improved by increasing the stiffness and diameter of the vibrating disks transmitting the motion of the projectors to the water body.

In situ motion of the swimbladder and otoliths:

As expected, the displacement of the auditory structures (e.g. otoliths) decreased with decreasing sound (pressure/particle motion) levels for both conditions, i.e. 0° and 180° (Fig. 2B). In both species, the otophysic connection led to an increase in otolith displacement (saccular otolith in both species; utricular otolith only in *E. canarensis*, Fig. 2C) when the animal was subjected to the in phase ("high" sound pressure) condition. The saccular otolith in goldfish and *E. canarensis* showed a complex motion pattern including a tilting movement relative to the rostrocaudal axis. The saccular ootlith in goldfish showed only a weak movement along the rostrocaudal but a strong motion alsong the dorsoventral axis although sound impinged along the rostrocaudal axis. In accordance with previously stated hypotheses (e.g. [9,10], the shape of the fragile saccular otoliths including thin wings seem to play an important role for the specific motion pattern of this otolith. Left and right otoliths of the same type showed differed in their motion when the sound impinged on the body flanks ("frontal view") during the out of phase condition whereas their motion pattern was indentical (mirror-imaged) during the in phase condition.
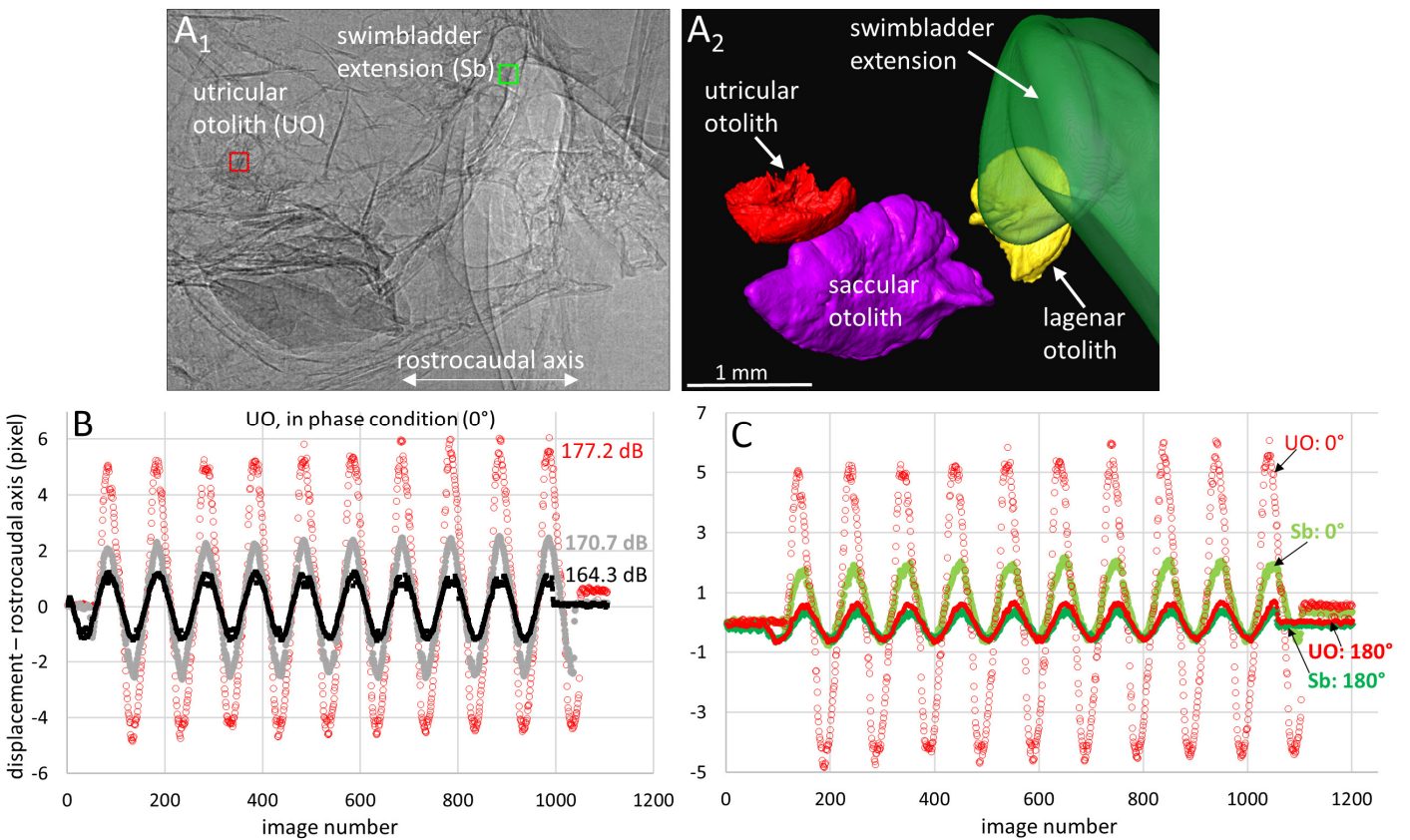

Fig. 2. (A$_1$) 2D radiograph of the otoliths and anterior swimbladder extensions in *E. canarensis* in lateral view. (A$_2$) 3D reconstructions of the otoliths and the swimbladder extensions. (B) Displacement plot depicting the motion of the utricular otolith along the rostrocaudal (x-) axis at three different sound pressure levels when the fish was subjected to the in phase condition. Decreasing sound pressure levels correlate with decreasing displacement of the otolith. (C) Displacement plot depicting the motion of the utricular otolith and the anterior swimbladder extension when the fish was subjected to the in phase (0°; 177.2 dB re 1 µPa) or out of phase condition (180°; 155.4 dB re 1 µPa), respectively. The displacement of both structures is distinctly smaller at the 180° condition.

Sound-induced swim bladder motion during tomography:

It is still difficult to stabilize the fish during the tomography while providing enough degrees of freedom for the auditory structures to move. It turned out that the fish is prone to slip downwards in the tube during sound presentation which makes it almost impossible to interpret the blurred swim bladder walls in the image stack as a result of sound-induced motion while this motion might also be a result from a shift of the whole fish during the scanning procedure.

Conclusions

With the new standing wave tube-like setup, we were able to 1) conduct experiments separately under the sound pressure or sound-induced particle motion condition, 2) detailly characterize the interplay between ancillary auditory structures such as anterior swimbladder extensions (*E. canarensis*) or Weberian ossicles (goldfish) and the otoliths and 3) provide (first) experimental evidence for several formerly stated hypotheses on how different types of otophysic connections affect otolith motion. Currently, we are writing up our main findings of 2D radiography in a manuscript that is going to be submitted to PLoS Biology [11].

References

1. Chranilov NS. Beiträge zur Kenntnis des Weber'schen Apparates der Ostariophysi 1. Vergleichend-anatomische Übersicht der Knochenelemente des Weber'schen Apparates bei Cypriniformes. Zool Jb Anat. 1927;49:501-97.
2. Schulz-Mirbach T, Heß M, Metscher BD, Ladich F. A unique swim bladder-inner ear connection in a teleost fish revealed by a combined high-resolution microCT and 3D histological study. BMC Biol. 2013;11:75.
3. Dehadrai PV. On the swimbladder and its connection with the internal ear in family Cichlidae. Proc Nat Inst Sci India B. 1959;25(5):254-61.
4. Ladich F, Fay RR. Auditory evoked potential audiometry in fish. Rev Fish Biol Fish. 2013;23:317-64.
5. Braun CB, Grande T. Evolution of peripheral mechanisms for the enhancement of sound reception. In: Webb JF, Fay RR, Popper AN, editors. Fish Bioacoustics. Springer Handbook of Auditory Research. New York: Springer; 2008. p. 99-144.
6. Schulz-Mirbach T, Olbinado M, Rack A, Mittone A, Bravin A, Melzer RR, et al. In-situ visualization of sound-induced otolith motion using hard X-ray phase contrast imaging. Sci Rep. 2018;8:3121.
7. Hawkins AD, MacLennan DN. An acoustic tank for hearing studies on fish. In: Schuijf A, Hawkins AD, editors. Sound reception in fish. Amsterdam: Elsevier; 1976. p. 149-69.
8. Hawkins AD. Underwater sound and fish behaviour. In: Pitcher TJ, editor. Behaviour of Teleost Fishes. London: Chapman and Hall; 1993. p. 129-69.
9. von Frisch K. Über die Bedeutung des Sacculus und der Lagena für den Gehörsinn der Fische. Zeitschr vgl Physiol. 1938;25:703-47.
10. Popper AN, Platt C. Sensory surface of the saccule and lagena in the ears of ostariophysan fishes. J Morphol. 1983;176(2):121-9.
11. Schulz-Mirbach T, Ladich F, Mittone A, Olbinado M, Bravin A, Maiditsch IP, et al. Auditory chain reaction: effects of sound pressure and particle motion on auditory structures in fishes. PLoS Biol. in prep.